MICROSTRUCTURAL EVOLUTION AND HARDNESS PROPERTIES OF Si-MODIFIED ALUMINIDE COATING ON 304 STAINLESS STEEL VIA SLURRY ALUMINIZING: EFFECT OF ALUMINIZING TEMPERATURES

Ibrahim Owolabi Ambali[1,2], Anasyida Abu Seman[1,*] and Tuti Katrina Abdullah[1]

[1]School of Materials and Mineral Resources Engineering, Universiti Sains Malaysia, 14300 Nibong Tebal, Pulai Pinang, Malaysia.
[2]Department of Materials & Metallurgical Engineering, University of Ilorin, Ilorin, Nigeria.

*anasyida@usm.my

Abstract. Surface modification of austenitic steel with a Si-modified aluminide coating enhances its lifespan by improving resistance to corrosion, oxidation, and high-temperature strength. To achieve this, a slurry composed of silicon, alumina, and aluminium was applied on the surface of 304 stainless steel (304SS) substrates. The samples were subjected to aluminizing at 750 °C, 800 °C, and 850 °C for 6 hours. Microstructural analysis was carried out using a field scanning electron microscope (FESEM) equipped with energy-dispersed X-ray spectroscopy (EDX), while X-ray diffraction (XRD) was employed for phase identification. The hardness of the coating was measured using Vicker microhardness. The study revealed the presence of various binary intermetallic compounds, including Fe_2Al_5, Fe_3Al, and FeAl, as well as ternary phases like $Al_3Fe_2Si_3$ and $Fe_{1.7}Al_4Si$, within the coatings. The addition of silicon reduced the intermetallic compound (IMC) layer thickness by occupying vacancy sites along the crystal structure c-axis of Fe_2Al_5, thereby restraining the growth of this brittle IMC in favor of more ductile phases. Notably, specimens heat treated at 850 °C exhibited the highest thickness of Fe-Al IMC layers. As temperature increases, the number of voids at the interface between the aluminide layer and the steel substrate also grew. Microhardness measurement revealed that Fe_2Al_5, FeAl, and Fe_3Al layers had a hardness value of about 850-990 HV, 570-630 HV, and 320-410 HV respectively for all the temperatures. Fe_2Al_5 has the lowest toughness and is confirmed to be the hardest zone in the aluminide coating. Si-modified aluminide coatings on 304 stainless steels could be considered as a material candidate for high temperature application.

Keywords: Si-modified aluminide coating, alumina, intermetallic layer, 304 stainless steel

Article Info

Received 4th January 2024
Accepted 23rd May 2024
Published 12th June 2024

ISSN: 1823-7010, eISSN: 2600-7444

1. INTRODUCTION

The introduction of protective coatings with aluminium on the surface of steel offers an effective solution to mitigate oxidation and corrosion resistance of steel for high temperature applications [1]. Aluminide coating is an exothermic reaction that involves the diffusion of aluminium into the substrate material by generating a fine and dense alumina scale and the formation of intermetallic compounds which significantly alter the surface characteristics of the base material by enhancing wear, oxidation, and corrosion properties of the steel. Aluminizing processes can be achieved through the following techniques such as pack aluminizing, hot dip aluminizing (HDA), physical vapour deposition (PVD), chemical vapor deposition (CVD), and slurry-based methods [2–5]. However, slurry has been considered as the most effective and reliable technique due to its simplicity, reparability, ease to manufacture and flexibility [6].

There are challenges associated in developing a protective aluminide coating layer due to depletion of aluminium during the interdiffusion between the coating and substrate which resulted in the formation of brittle Fe-Al intermetallic layer such as Fe_2Al_5 and $FeAl_3$ with an irregular shape (tongue-like) morphology due to vacancy site exist in the c-axis of the crystal structure of Fe_2Al_5 that act as a stress concentrator. The initiation of crack due to thermal expansion coefficient (CTE) mismatch between intermetallic layers and substrate deteriorates the mechanical proprieties of the coating layers which increases corrosion and oxidation rate. However, the Al_2O_3 layer that is developed on the surface of the coating has a tendency to undergo spalling when subjected to cyclic oxidation at elevated temperatures [7].

The microstructure plays a significant role in determining the mechanical properties of any material and the evolution of the microstructure in the aluminide layer alters the hardness properties of the aluminide steel and influences the service life of the aluminized steel. Optimising the process parameters such as temperature, time and adding alloying elements are essential to control the microstructure and growth rate of the intermetallic layers [8].

Modification of aluminide coating with silicon addition impedes the inward diffusion rate of aluminium activities by occupying the vacancy in the c-axis of the Fe-Al intermetallic layer thereby suppressing the growth rate of Fe_2Al_5, smoothing the irregular morphology and transforming the phase constitution from Fe-Al binary phases to Fe-Al-Si ternary phase [9-10].

Zarei et al. [11] and other authors, Cheng and Wang [12] observed the phase transformation of intermetallic layer into a flat morphology with addition of silicon in aluminium bath. Evidence showed that the thickness of the intermetallic compound (IMC) layer decreased significantly with increasing Si. They also found that Al_7Fe_2Si and $Al_2Fe_3Si_3$ are formed adjacent to the intermetallic layers of Fe_2Al_5 and $FeAl_3$. Also, Ma et al. [13] and Zou et al. [14] investigated the effect of Si content on the growth of IMC layers at a relatively wide temperature. They observed the reduction in the IMC layers with the disappearance of irregular interface between the coating and substrates and suggested the formation of ternary phases of Fe-Al-Si segregated within IMC layers.

Despite various studies on the above subject, there is still a lack of research on the effect of varying silicon contents and aluminizing temperatures on 304SS. Thus, this research aim is to investigate the microstructural evolution of the intermetallic layer formed and hardness properties of the silicon-alumina-aluminium coating on 304SS via slurry aluminizing at different aluminizing temperatures.

2. MATERIALS AND METHODS

2.1 Material

The substrate used for this experiment is Austenitic stainless steel of grade 304. The material was cut into dimensions 10 mm x 10 mm x 2 mm which was then mechanical ground with 180 grit of silica carbide paper under flowing water to make a rough surface for quality slurry adhesion. To remove grease and oxides from the surface of the specimen, the specimens were ultrasonically cleaned in an acetone solution. Then followed by dipping in a NaOH solution and pickled in a solution of HCl for one minute each and washed in distilled water. The specimen is then allowed to dry for 30 minutes.

2.2 Slurry Preparation and Coating

The slurry was prepared by percentage mixing ratio of 57% of solvent consist of distilled water and PVA 14000 as binder and 43% additives [15]. The additives compose of percentage mixing ratio of the powders (70% Al, 15% Al_2O_3, and 15% Si). The prepared slurry was sprayed on all the surfaces and edges of the sample with the aid of Sagola gun attached to the air pressure for applying slurry on the substrates. The coating procedure was controlled to achieve a mass/area of 15-30 mg. The coated samples were then left to dry in laboratory air for 1 hour. Diffusion aluminizing was conducted in a carbolite tube furnace under the argon environment. The aluminizing was done at various temperatures 750, 800 and 850 °C for 6 hours.

2.3 Coating Characterization

Metallurgical examination was conducted on the aluminide samples by mounting the samples in an epoxy resin, ground with various silica carbide paper in the grade 240-2000 grits and finally polished into a mirror like with alumina paste up to 0.05 μm and etched with a standard Keller etchant reagent for 3-5 s to reveal the microstructures of the samples. Surface morphology, cross sectional microstructure and chemical composition were analyzed by a FESEM (ZEISS SUPRA 35VP) with Energy Dispersive X- ray Spectrometer (EDX; Edax Ametex Z2 analyzer). X-ray diffraction (XRD Bruker Advanced D8) with Cu Kα radiation (λ = 0.15406 nm) and 2θ scanning from 10° to 100° was also performed on the samples for phases identification. Microhardness (LECO micro-indentation hardness tester LM248AT) was performed on the coating's samples under the load of 25 g for 15 s. Coating thickness of IMC layers were measured using Image J software on FESEM Image.

3. RESULTS AND DISCUSSION

3.1 Surface Image

Figure 1(a) shows the pictorial image of the sample after heated at 850 °C for 6 hours. The image demonstrated that the surface of the substrate was fully covered with coating layers with dark appearance after heat treated. The dark appearance indicated the alumina scale formed during the aluminizing process. Figure 1(b) shows the surface morphology representing the heat-treated sample. The image revealed grains size uniformly distributed. Al_2O_3 and SiO_2 are randomly distributed within the layers which serve as the protect oxides scale for the aluminized stainless steel at high temperatures. While Figure 1(c) shows a cross sectional of the aluminide coating layer.

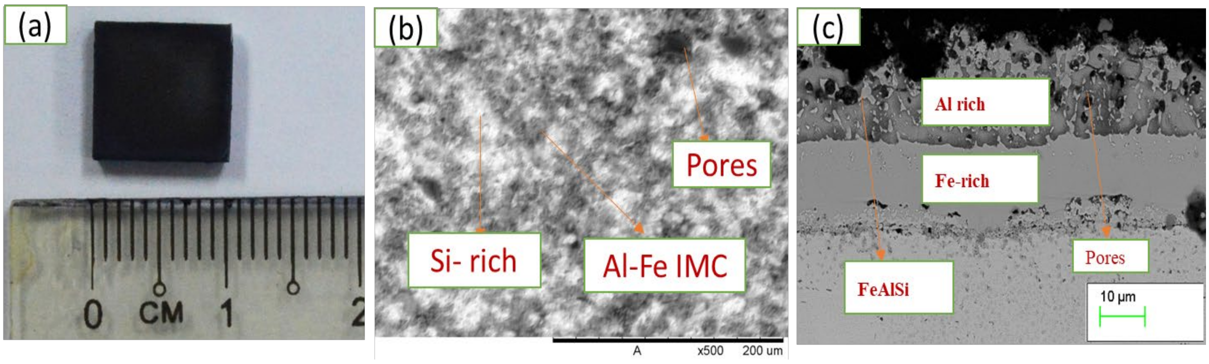

Figure 1: a) Pictorial image of aluminide coating, b) Surface Morphology of the aluminide coating and c) Cross section image of the aluminide coating

3.2 Microstructure and Phase Transformation in the Aluminide Layer

Figures 2, 3 and 4 show the cross-sectional images of modified aluminide coating at 750, 800 and 850 ºC for 6 hours. The images revealed the two-layer structures on the coating layer namely: i) outer layer with rough surface also known as diffusion zone, while ii) inner layer consists of fine and continuous layer known as interdiffusion zone (IDZ) formed during the aluminizing process at different aluminizing temperatures. During the interdiffusion between the coating and substrate, the reaction layers are continuous but vary in thickness along the interface. Additionally, the morphology of the interfaces towards the adjacent base materials changes with temperatures. The outer layers was rich in aluminium while the inner layer was rich in Fe with ternary phases segregated out in the coating during the reaction between the modified aluminium-silicon from the coating and Fe from the substrate. Researchers have confirmed the segregation of AlFeSi IMC manifested at the AlSi bath and the substrates [11-12,16]. Pores are found at the IMC layers which are formed due to Kirkendall effect where a net flux of vacancies on the protruding isolated serrated steel is caused by different Fe and Al diffusion rates, which then condense out into voids. The void was also caused by uneven volume shrinkage during transition from Fe_2Al_5 into FeAl. However, the increase in pores is attributed to the increase in aluminizing temperatures which resulted in the suppress growth of Fe_2Al_5. Sun et al. [17], Chang & Rock [18] and some researchers observed the presence of voids in the layers as the treatment temperature increases which also match with this work. Based on the EDX and line scan analysis, chemical compositions of the aluminide layers were quantified at different points on the coating layers by the percentage ratio of Al, Fe and Si at atomic % with the corresponding concentration of aluminium, silicon, and Fe during the aluminizing. The phases appeared in the EDX analysis consist of both binary and ternary intermetallic phases namely; Fe_2Al_5, $FeAl_3$, FeAl, Fe_3Al, $Fe_2Al_3Si_3$ and $Fe_{1.7}Al_4Si$ respectively at the spot area on different location points as indicated on the images shown in the Figures 2, 3 and 4. This observation is in accordance with previous studies [10,13].

The results of EDX revealed the Fe-Al intermetallic phase consist of major phases of Fe_2Al_5 which is first to form due to the smallest free energy during the interdiffusion while the regions at the topcoat, aluminium concentration increased to the value correspond to $FeAl_3$. The region close to the substrate are FeAl and Fe_3Al while addition of silicon involved in the intermetallic formation of Fe-Al-Si. The phases appeared in the EDX analysis consist of both binary and ternary intermetallic phases namely; Fe_2Al_5, $FeAl_3$, FeAl, Fe_3Al, $Fe_2Al_3Si_3$ and $Fe_{1.7}Al_4Si$ respectively at the spot area on different location points as indicated on the images shown in the Figures 2, 3 and 4. This observation is in accordance with previous studies [10,13].

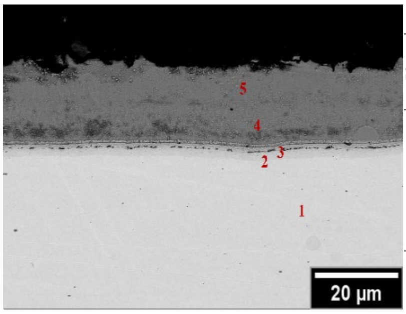

Spots	Composition (at.%)		for 750°C at 6hr			
	Fe	Al	Si	Cr	Ni	O
1	65.82	1.48	2.1	20.26	7.65	2.68
2	44.09	28.85	5.88	11.87	7.36	1.95
3	28.86	44.04	19.93	3.83	1.85	1.48
4	20.43	63.25	8.97	3.23	2.63	1.5
5	17.92	57.38	18.85	2.76	1.3	1.79

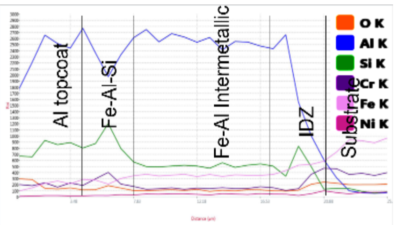

Figure 2: FESEM micrographs of cross-sectional image, corresponding EDX and line scan concentration profile of Si-modified aluminide coating on 304SS at 750 °C for 6 hours

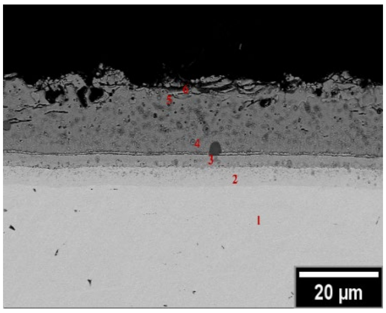

Spots	Composition (at. %)		for 800°C at 6 hr			
	Fe	Al	Si	Cr	Ni	O
1	71.29	1.38	2.1	22.55	7.35	2.68
2	65.72	7.1	4.29	19.31	3.68	3.58
3	38.53	38.57	14.65	5.2	3.98	3.06
4	14.58	44.82	10.92	10.18	4.76	19.5
5	22.94	53.32	21.16	1.4	3.92	1.9
6	32.47	58.2	12.48	3.94	2.81	6.22

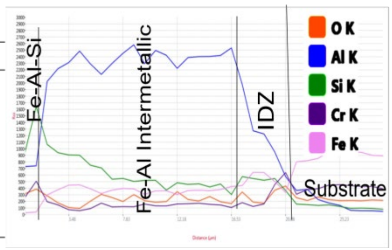

Figure 3: FESEM micrographs of cross-sectional image, corresponding EDX and line scan concentration profile of Si-modified aluminide coating on 304SS at 800 °C for 6 hours

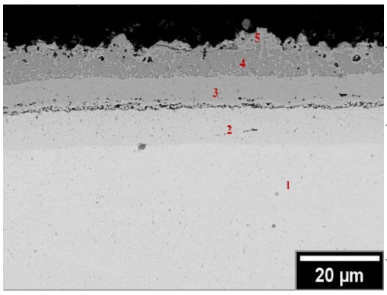

Spots	Composition (at. %)		for 850°C at 6 hr			
	Fe	Al	Si	Cr	Ni	O
1	64.57	6.05	3.88	19.59	3.56	2.35
2	55.35	21.84	3.74	11.32	5.25	2.51
3	35.25	33.31	16.53	8.56	4.24	2.1
4	21.89	62.11	6.75	3.92	3.73	1.6
5	23.11	61.53	5.94	3.71	3.54	2.18

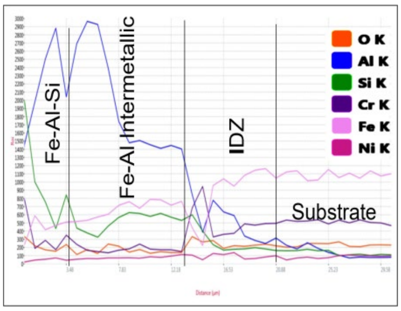

Figure 4: FESEM micrographs of cross-sectional image, corresponding EDX and line scan concentration profile of Si-modified aluminide coating on 304SS at 850 °C for 6 hours

Figure 5 shows the IMC detected by the XRD at 750, 800 and 850 °C. The phases detected include the following phases: Fe_2Al_5 with (ICDD PDF number: 00-029-0043), FeAl (ICDD PDF number: 04-013-5555) and Fe_3Al (ICDD PDF number: 04-013-9780). All these phases are the primary phases, but the absence of $FeAl_3$ phase could be attributed either weak peak or too small be detected by the XRD. The ternary phases detected includes: $Fe_{1.7}Al_4Si$ (ICDD PDF number: 04-008-4784) and $Fe_2Al_3Si_3$ (ICDD PDF number: 01-984-4861). The results agreed with Ma et al. [13].

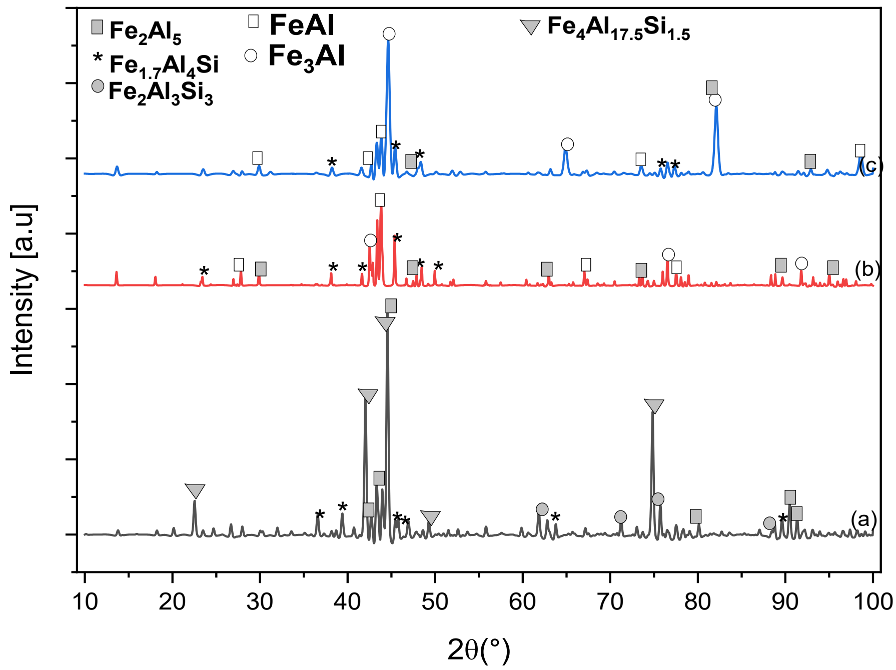

Figure 5: XRD pattern of Si modified aluminide coating on 304SS at a) 750 ˚C, b) 800 ºC and c) 850 ˚C for 6 hours

3.3 Coating Thickness

Figure 6 shows the trend of thickness of the aluminide coating layers at different aluminizing temperatures. As temperatures increases, the Fe_2Al_5 layers decrease, sample heat treated at 750 ℃ has the highest thickness of Fe_2Al_5 with the least recorded at 850 ºC while the FeAl layers increase as the temperature increases. FeAl layer could be responsible for corrosion resistance of the aluminide coating on 304SS. The decrease in Fe_2Al_5 layer and the formation of voids within the IMC result from the prolonged exposure to higher temperatures during the aluminizing, leading to increase of diffusion. Sample heat treated at 750 °C has the least coating thickness of FeAl layer with thickness value of 1.66 µm + 0.25 µm, This result is in accordance with the previous studies [19]. However, the presence of Fe-Si-Al has a significant role in keeping the thickness of the IMC (Fe_2Al_5) layer to a minimum. The addition of silicon reduced IMC (Fe_2Al_5) layer thickness by occupying vacancy sites along the crystal structure c-axis of Fe_2Al_5 forming Fe-Si-Al phase.

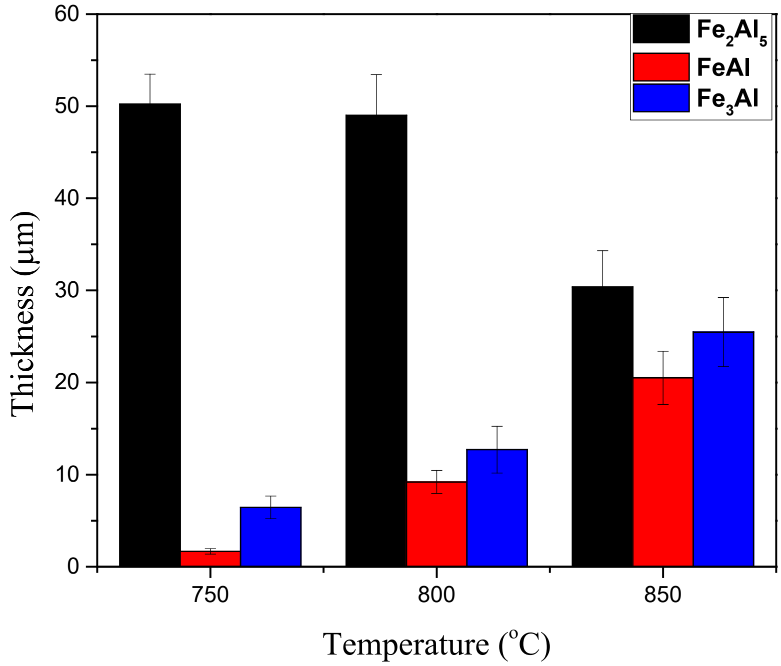

Figure 6: Coating thickness of the Si-modified aluminide coating on 304SS for 6 hours at 750, 800 and 850 ºC

3.4 Hardness Properties

The hardness values of the modified aluminide coating at 750, 800 and 850 ºC is shown in Figure 7. The hardness values of Fe_2Al_5 ranges between 850-880 HV, FeAl has the hardness values ranges between 570-630 HV, and the hardness value of Fe_3Al ranges between 320-410 HV. Sample heat treated at 850 ºC for 6 h has the maximum hardness value of 880 HV for Fe_2Al_5 phase while the minimum value of Fe_2Al_5 phase was recorded at 750 ºC with hardness value of 850 HV. The increase in hardness is attributed to the increase in prolonged aluminizing temperatures. Fe_3Al has the lowest hardness value near the substrate. The phase is formed at a temperature below 400 °C with a free energy greater than zero. This phase has the highest ductility, and the formation mechanism is listed below [2].

$$2\text{Fe} + 5[\text{Al}] \rightarrow Fe_2Al_5 \quad (1)$$

$$Fe_2Al_5 + [\text{Al}] \rightarrow 2\text{Fe}Al_3 \quad (2)$$

$$Fe_2Al_5 + 3\text{Fe} \rightarrow 5\text{FeAl} \quad (3)$$

$$3\text{Fe} + [\text{Al}] \rightarrow Fe_3\text{Al} \quad (4)$$

Fe_2Al_5 phase was firstly formed due to the rapid infiltration of Al atom towards the substrate (equation 1). Subsequently, Fe_2Al_5 reacts with Al atoms to produce $FeAl_3$ (equation 2). Near the substrate, Fe atoms diffuse outward towards Fe_2Al_5, resulting in the formation of FeAl and Fe_3Al phases according to equations 3 and 4. Fe_2Al_5 and $FeAl_3$ are brittle IMC. They have low toughness and high corrosion rate which is detrimental to the mechanical properties of the 304SS. While FeAl and Fe_3Al are ductile phases that are required to protect the 304SS for high temperature corrosion resistance.

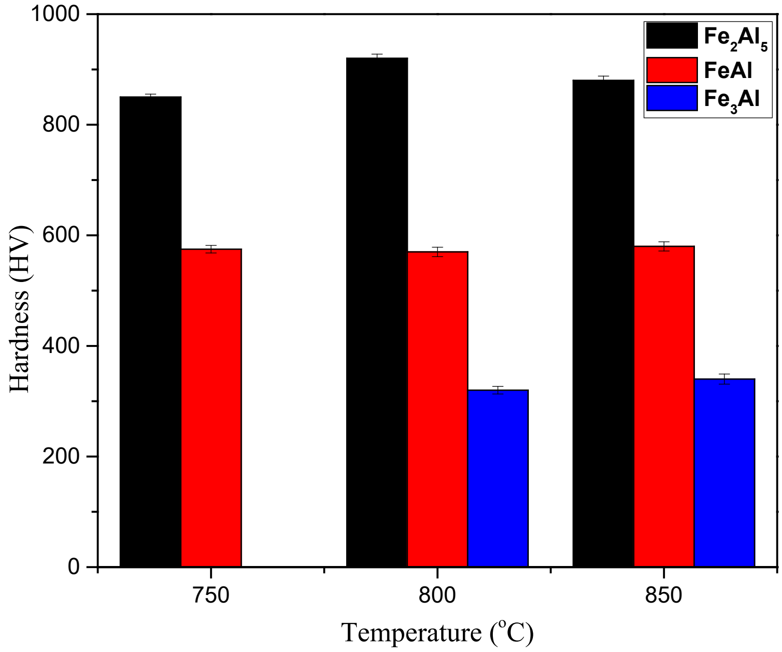

Figure 7: Hardness of Si modified aluminide coating layers on 304SS for 6 hours at 750, 800 and 850 °C.

4. CONCLUSIONS

The alumina-silicon modified aluminide coatings were successfully developed on the 304SS through the slurry technique at 750, 800 and 850 °C for 6 hours. Aluminizing produced a coating layer consisting mainly of Fe_2Al_5, FeAl and Fe_3Al. In addition, Fe-Al-Si intermetallic ($Fe_{1.7}Al_4Si$ and $Fe_2Al_3Si_3$) phases were also found in the modified aluminide coating layer. The formation of a continuous and dense Fe-rich intermetallic layer on Si-modified coating exhibited a lower coating hardness as compared to the Al-rich intermetallic layer. The addition of Si on aluminide coating effectively reduced the thickness of brittle IMC (Fe_2Al_5 and $FeAl_3$) and promotes the growth of FeAl, and Fe_3Al layers. This can improve corrosion resistance at high- temperature applications.

Acknowledgements

The author gratefully acknowledges the School of Materials and Mineral Resources Engineering, Universiti Sains Malaysia for facilities provided and funding provided by Ministry of Higher Education Malaysia for Fundamental Research Grant Scheme (FRGS) with Project Code: FRGS/1/2021/TK0/USM/02/22 and the sponsorship by TETFund, Nigeria (TETF/ES/UNIV/KWARA/TSAS/ 2021).

Author Contributions

Ibrahim Owolabi Ambali: investigation, methodology, writing - original draft. Anasyida Abu Seman: supervision, conceptualization, writing - review and editing, methodology, funding acquisition. Tuti Katrina Abdullah: conceptualization, supervision.

Disclosure of Conflict of Interest

The authors declare that they have no known competing financial interests or personal relationships that could have appeared to influence the work reported in this paper.

Compliance with Ethical Standards

The work is compliant with ethical standards.

References

[1] Bauer, J.T., Montero, X. & Galetz, M.C. (2020). Fast heat treatment methods for al slurry diffusion coatings on alloy 800 prepared in air. *Surface and Coatings Technology*. 381, 125140.

[2] Dong, J., Sun, Y. & He, F. (2019). Formation mechanism of multilayer aluminide coating on 316L stainless steel by low-temperature pack cementation. *Surface and Coatings Technology*, 375, 833–838.

[3] Prasanthi, T. N., Sudha, C. & Reddy, P. S. (2022). Hot dip aluminization of 304L SS and P91 ferritic-martensitic steel – Comparison of interface morphology and growth kinetics of reaction zones. *Surface and Coatings Technology*, 440, 128465.

[4] Ardigo-Besnard, M. R., Popa, I. & Chevalier, S. (2019). Effect of spinel and perovskite coatings on the long term oxidation of a ferritic stainless steel in H2/H2O atmosphere. *Corrosion Science*, 148, 251–263.

[5] Triani, R. M., Gomes, L. F. D. A., Aureliano, R. J. T., Neto, A. L., Totten, G. E. & Casteletti, L. C. (2020). Production of Aluminide Layers on AISI 304 Stainless Steel at Low Temperatures Using the Slurry Process. *Journal of Materials Engineering and Performance*, 29(6), 3568–3574.

[6] Soleimani Dorcheh, A. & Galetz, M. C. (2016). Slurry aluminizing: A solution for molten nitrate salt corrosion in concentrated solar power plants. *Solar Energy Materials and Solar Cells*, 146, 8–15.

[7]Cheng, W. J. & Wang, C. J. (2013). High-temperature oxidation behavior of hot-dipped aluminide mild steel with various silicon contents. *Applied Surface Science*, 274, 258–265.

[8]Singhal, P. & Saxena, K. K. (2019). Effect of silicon addition on microstructure and mechanical properties of grey cast Iron: An overview. *Materials Today: Proceedings*, 26,

1393–1401.

[9] Lemmens, B., Springer, H., De Graeve, I., De Strycker, J., Raabe, D. & Verbeken, K. (2017). Effect of silicon on the microstructure and growth kinetics of intermetallic phases formed during hot-dip aluminizing of ferritic steel. *Surface and Coatings Technology*, 319, 104–109.

[10] Cheng, W. J. & Wang, C. J. (2010). Observation of high-temperature phase transformation in the Si-modified aluminide coating on mild steel using EBSD. *Materials Characterization*, 61(4), 467–473.

[11] Zarei, F., Nuranian, H. & Shirvani, K. (2020). Effect of Si addition on the microstructure and oxidation behaviour of formed aluminide coating on HH309 steel by cast-aluminizing. *Surface and Coatings Technology*, 394, 125901.

[12] Cheng, W. J. & Wang, C. J. (2011). Microstructural evolution of intermetallic layer in hot-dipped aluminide mild steel with silicon addition. *Surface and Coatings Technology*, 205(19), 4726–4731.

[13] Ma, Y., Yuan, B., Liu, Y., Wang, J. & Su, X. (2022). Effect of Annealing and oxidationon the Microstructure Evolution of Hot-Dipped Aluminide Q345 Steel with Silicon Addition. *MDPI Coatings*, 503(12), 1-15.

[14] Zou, T. P., Yu, G. Y., Chen, S. H., Huang, J. H., Jian, Y. A. N. G., Zhao, Z. Y., Rong, J. P. & Jin, Y. A. N. G. (2021). Effect of Si content on interfacial reaction and properties between solid steel and liquid aluminum. *Transactions of Nonferrous Metals Society of China*, 31(9), 2570-2584.

[15] Boulesteix, C. & Pedraza, F. (2018). Characterisation of aluminium diffusion coatings elaborated on austenitic stainless steels and on ferritic-martensitic steels. *Surface and Coatings Technology*, 339, 27–36.

[16]Wang, H., Sun, S., Li, X., Wang, J. & Su, X. (2022). Effect of silicon on interfacial reaction and morphology of hot-dip aluminizing. *Journal of Materials Research and Technology*, 20, 3723–3734.

[17] Sun, Y., Dong, J., Zhao, P. & Dou, B. (2017). Formation and phase transformation of aluminide coating prepared by low-temperature aluminizing process. *Surface and Coatings Technology*, 330, 234–240.

[18] Chang, Y. Y., Tsaur, C. C. & Rock, J. C. (2006). Microstructure studies of an aluminide coating on 9Cr-1Mo steel during high temperature oxidation. *Surface and Coatings Technology*, 200, 6588–6593.

[19] Abu Kassim, S., Muzirah, M. S., Ahmad, Z. S., Abu Seman, A. & Abdullah, K. T. (2021). Si-Mo-Modified Aluminide Slurry Coating For High Temperature Protection of Austenitic Stainless Steel. *Malaysian Journal of Microscopy,* 17(2), 88-99.